Synthesis and Characterization of a Neutral Tricoordinate Organoboron Isoelectronic with Amines

Rei Kinjo, *et al.*

Science **333**, 610 (2011);
DOI: 10.1126/science.1207573

between the tip and graphene. Puckering deformation due to the tip pushing the ripple crest forward along the scanning direction explains the 180° anisotropy. Therefore, if Θ is the relative angle between the ripple line and the scan direction, we can then expect minima and maxima separated by 90° with an angular dependence following a |sin Θ| relation, because the in-plane force component along the direction perpendicular to the ripple line of the AFM tip varies in this way.

A high loading force induces a large contact area (100 to 1000 nm^2), which can decrease the relative contribution of ripple deformations to the friction and thus the dependence on Θ. This is because puckering takes place at the exposed graphene in contact proximity to the tip (Fig. 4C). Although the contact area increases at the high load, the contribution of the ripple deformation around the tip in relation to the contact area decreases, and thus the bending of graphene becomes less dependent on the scan direction. We can expect, therefore, more isotropic puckering and friction at the high load. High-resolution friction images showed the existence of lattice distortions that could be associated with the puckering (fig. S1). These distortions were not observed on bulk graphite images obtained under identical conditions. Because bulk graphite can be considered an extremely thick graphene, such distortion associated with puckering seems to decrease as the graphene thickness increases.

As a further test of this model, we performed FFM measurements on a graphene sheet accidentally deposited over a particle in the substrate. The images revealed mechanical wrinkles and friction domains induced by stress in the proximity of the particle (figs. S2 and S3). Ripples created by the radial stress around the particle are manifested in the formation of domains exhibiting friction anisotropy with similar 180° periodicity (Fig. 2). The 60° shift between ripple lines of adjacent domains supports our assumption that the ripple lines are related to the crystallographic direction of the graphene. The friction contrast in the domains also became weaker after thermal annealing at 200°C and disappeared completely after annealing at 400°C (fig. S4). The initial anisotropy was a characteristic of the graphene flake previous to equilibration. Because two-dimensional structured graphene has a negative thermal expansion coefficient, heating and cooling processes can restore the graphene to equilibrium, changing a stress-induced ripple (*4*).

Our results indicate that friction mapping on the graphene layer constitutes a powerful tool to study the ripple structure formed on graphene during mechanical exfoliation processes. Another interesting outcome of our research is that the control of friction and anisotropic mechanical properties, such as the one presented here with a large anisotropy ratio of 215%, could be exploited in solid lubrication of micro- or nanoelectromechanical systems.

References and Notes

1. K. S. Novoselov *et al.*, *Science* **306**, 666 (2004).
2. A. Hashimoto, K. Suenaga, A. Gloter, K. Urita, S. Iijima, *Nature* **430**, 870 (2004).
3. A. Fasolino, J. H. Los, M. I. Katsnelson, *Nat. Mater.* **6**, 858 (2007).
4. W. Bao *et al.*, *Nat. Nanotechnol.* **4**, 562 (2009).
5. K. Xu, P. Cao, J. R. Heath, *Nano Lett.* **9**, 4446 (2009).
6. C. H. Lui, L. Liu, K. F. Mak, G. W. Flynn, T. F. Heinz, *Nature* **462**, 339 (2009).
7. P. Y. Huang *et al.*, *Nature* **469**, 389 (2011).
8. J. Y. Park, P. A. Thiel, *J. Phys. Condens. Matter* **20**, 314012 (2008).
9. C. Lee *et al.*, *Phys. Status Solidi B* **246**, 2562 (2009).
10. C. Lee *et al.*, *Science* **328**, 76 (2010).
11. H. Lee, N. Lee, Y. Seo, J. Eom, S. W. Lee, *Nanotechnology* **20**, 325701 (2009).
12. T. Filleter *et al.*, *Phys. Rev. Lett.* **102**, 086102 (2009).
13. A. C. Ferrari *et al.*, *Phys. Rev. Lett.* **97**, 187401 (2006).
14. J. Y. Park, D. F. Ogletree, P. A. Thiel, M. Salmeron, *Science* **313**, 186 (2006).
15. D. S. Grierson, E. E. Flater, R. W. Carpick, *J. Adhes. Sci. Technol.* **19**, 291 (2005).
16. M. Dienwiebel *et al.*, *Phys. Rev. Lett.* **92**, 126101 (2004).
17. J. Y. Park *et al.*, *Science* **309**, 1354 (2005).
18. M. Liley *et al.*, *Science* **280**, 273 (1998).
19. R. W. Carpick, D. Y. Sasaki, A. R. Burns, *Tribol. Lett.* **7**, 79 (1999).
20. K. Min, N. R. Aluru, *Appl. Phys. Lett.* **98**, 013113 (2011).
21. A. Sakhaee-Pour, *Solid State Commun.* **149**, 91 (2009).
22. S. V. Morozov *et al.*, *Phys. Rev. Lett.* **97**, 016801 (2006).

Acknowledgments: Supported by the National Research Foundation of Korea funded by the Ministry of Education, Science, and Technology (National Research Laboratory program grant 2008-0060004; World Class University program grants R31-2008-000-10057-0 and R31-2008-000-10055-0; Basic Science Research program grants KRF-2008-314-C00111, KRF-2010-0005390, 2010-0015035, 2011-0014209, and 2011-0017605; and Quantum Metamaterials Research Center grant R11-2008-053-03002-0). M.B.S. was supported by the Office of Basic Energy Sciences, Division of Materials Sciences and Engineering, U.S. Department of Energy, under contract DE-AC02-05CH11231. J.S.C. was supported by a Hi Seoul Science/Humanities Fellowship from the Seoul Scholarship Foundation.

Supporting Online Material

www.sciencemag.org/cgi/content/full/science.1207110/DC1
Materials and Methods
Figs. S1 to S4
References

18 April 2011; accepted 16 June 2011
Published online 30 June 2011;
10.1126/science.1207110

Synthesis and Characterization of a Neutral Tricoordinate Organoboron Isoelectronic with Amines

Rei Kinjo,[1] Bruno Donnadieu,[1] Mehmet Ali Celik,[2] Gernot Frenking,[2] Guy Bertrand[1]*

Amines and boranes are the archetypical Lewis bases and acids, respectively. The former can readily undergo one-electron oxidation to give radical cations, whereas the latter are easily reduced to afford radical anions. Here, we report the synthesis of a neutral tricoordinate boron derivative, which acts as a Lewis base and undergoes one-electron oxidation into the corresponding radical cation. These compounds can be regarded as the parent borylene (H-B:) and borinylium ($H\text{-}B^{+\cdot}$), respectively, stabilized by two cyclic (alkyl)(amino)carbenes. Ab initio calculations show that the highest occupied molecular orbital of the borane as well as the singly occupied molecular orbital of the radical cation are essentially a pair and a single electron, respectively, in the p(π) orbital of boron.

The chemistry of boron is dominated by compounds in which the element adopts the +3 oxidation state and acts as a potent electron pair acceptor, or Lewis acid. To compensate its intrinsic electron deficiency, boron also often participates in multicenter bonds, and numerous clusters involving hypervalent boron centers are known (*1*). At the opposite extreme, it is only recently that low-valent boron derivatives have been thoroughly explored (*2*–*9*). Among these species, borylenes (BR), the subvalent boron(I) derivatives analogous to carbenes (CR_2) and nitrenes (NR), have been spectroscopically characterized in solid inert gas matrices at temperatures of a few K (*10*, *11*) but to date have eluded preparative isolation. Nonetheless, Braunschweig *et al.* (*12*) have shown that borylenes can be incorporated into the ligand sphere of stable, isolable transition metal complexes (*13*).

In recent years, stable singlet carbenes such as N-heterocyclic carbenes (NHCs) (*14*, *15*) and cyclic (alkyl)(amino)carbenes (CAACs) (*16*) have proven as powerful as transition metal centers for stabilizing highly reactive main group element species (*17*, *18*). In the boron series, Robinson and co-workers (*19*, *20*) have reported that reduction of the (NHC)BBr_3 adduct **A** produced the isolable stable neutral diborene **B**, which can be regarded as a dimer of the parent borylene-

[1]UCR-CNRS Joint Research Chemistry Laboratory (UMI 2957), Department of Chemistry, University of California Riverside (UCR), Riverside, CA 92521–0403, USA. [2]Fachbereich Chemie, Philipps-Universitat Marburg, Hans-Meerwein-Strasse, 35032 Marburg, Germany.

*To whom correspondence should be addressed. E-mail: guy.bertrand@ucr.edu

carbene complex (Fig. 1). By using a similar synthetic approach, Braunschweig and co-workers (*21*) generated the parent borylene-carbene complex **D**, and, although they were not able to characterize it spectroscopically, trapping experiments left no doubt of its transient existence.

The extreme reactivity of borylenes is due to their two vacant orbitals as well as the presence of a lone pair of electrons. We reasoned that two carbene ligands might simultaneously decrease the Lewis acidity while also accepting sufficient electron density to diminish the Lewis basicity and thereby stabilize a borylene. Having already shown that CAACs are slightly more nucleophilic but considerably more electrophilic than NHCs (*22*–*24*), we considered them good candidates. Here, we report the isolation of the parent borylene supported by two CAACs. We show that this neutral tricoordinate organoboron, featuring boron in the +1 oxidation state, can be oxidized to afford the corresponding stable radical cation and even protonated to give the conjugate acid.

In order to be able to protect the boron center while still having space for coordination of two carbenes, we chose CAAC **1** (*25*), featuring a bulky 2,6-diisopropylphenyl group at nitrogen and a flexible cyclohexyl moiety as the second carbene substituent. The first CAAC was installed classically (*19*–*21*) by reaction of **1** with BBr_3 in hexane, which afforded the $(CAAC)BBr_3$ adduct **2** in 94% yield (*26*). Then, in the hope of trapping the putative (CAAC)BH adduct by a second CAAC, a fivefold excess of potassium graphite was added to 1/1 mixture of boron adduct **2** and CAAC **1** in dry toluene. The reaction mixture was stirred at room temperature for 14 hours, and, from a complex mixture of unidentified products, compound **3** was isolated as a red powder in only 8% yield (Fig. 2). Unexpectedly, when the same experiment was carried out in the absence of CAAC **1**, the $(CAAC)_2BH$ adduct **3** was also formed and isolated in 33% yield. The ^1H-decoupled ^{11}B nuclear magnetic resonance (NMR) spectrum of **3** shows a broad signal at 12.5 parts per million (ppm) with a half-width of 216 Hz. In the proton-coupled ^{11}B NMR spectrum, no clear splitting was observed, but a broadening of the signal with a half-width of 261 Hz was. The presence of the hydrogen atom at boron was confirmed by an infrared absorption at 2455 cm^{-1} (fig. S1), which can be assigned to the B-H stretching mode (*27*). Single crystals suitable for an x-ray diffraction study were obtained by recrystallization from a dry tetrahydrofuran (THF) solution at room temperature. In the solid state (Fig. 3, left), the carbene carbons C1 and C2, boron, and the hydrogen H1 are in a perfectly planar arrangement (sum of the bond angles at B is 359.94°). The B1-C1 [1.5175 ± 0.0015 Å] and B1-C2 [1.5165 ± 0.0015 Å] bond distances are equal and are halfway between typical B-C single (1.59 Å) and double (1.44 Å) bonds (*28*), suggesting the delocalization of the lone pair of electrons at boron to the empty p orbitals of the carbene centers. Ab initio calculations performed on **3** at the BP86/def2-SVP level of theory support this bonding analysis. The carbene→BH donation occurs from the σ lone pairs of carbene ligands into the empty in-plane molecular orbital at boron, affording two low-lying orbitals. The highest occupied molecular orbital (HOMO) of **3** (–3.34 eV) is essentially an electron lone pair in the p(π) orbital of boron, which mixes in a bonding fashion with the p(π) atomic orbital of the two carbene carbons (Fig. 4, left). The charge exchange via σ donation and π backdonation leaves the BH moiety in **3** with a partial charge of +0.05 *e*. For comparison, the BH fragment in $(CH_3)_2BH$, which has two B-C electron-sharing bonds, carries a positive charge of +0.61 *e*. Therefore, the zwitterionic form **3b**, featuring a dianionic boron center (*29*), is a far weaker resonance contributor than **3a**, which shows the parent borylene coordinated by two carbene ligands.

The boron in compound **3** is in the formal oxidation state +1 and is electron-rich. This was confirmed by the cyclic voltammogram (fig. S2) of a THF solution of **3** (0.1 M nBu_4NPF_6 electrolyte), which shows a reversible one-electron oxidation at $E_{1/2} = -0.940$ V versus Fc+/Fc (Fc is ferrocene). Indeed, addition at room temperature of two equivalents of gallium trichloride to a toluene solution of **3** quantitatively afforded the radical cation $[\mathbf{3}^{+\cdot}]GaCl_4^-$. A single crystal x-ray diffraction study showed that the boron center of $[\mathbf{3}^{+\cdot}]GaCl_4^-$ is in a perfectly planar arrangement, as observed for its precursor **3** (Fig. 3, center).

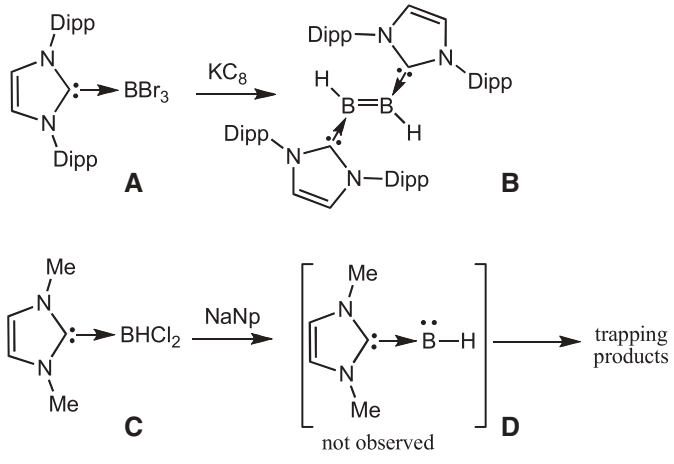

Fig. 1. (**Top**) Synthesis of the neutral bis(carbene)-stabilized diborene **B**, the dimer of the parent borylene-NHC adduct, by Robinson and co-workers (*19*, *20*) (Dipp indicates 2,6-diisopropylphenyl; Me, methyl group). (**Bottom**) Generation of a transient parent borylene-NHC adduct **D** by Braunschweig and co-workers (*21*) (Np, naphthalene).

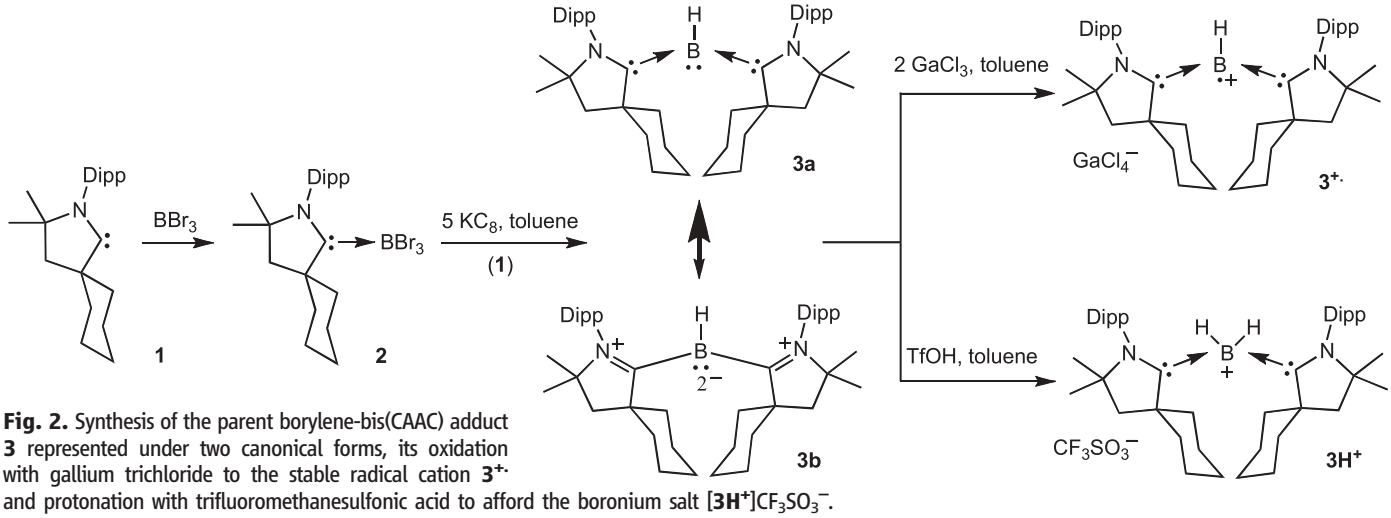

Fig. 2. Synthesis of the parent borylene-bis(CAAC) adduct **3** represented under two canonical forms, its oxidation with gallium trichloride to the stable radical cation $\mathbf{3}^{+\cdot}$ and protonation with trifluoromethanesulfonic acid to afford the boronium salt $[\mathbf{3H}^+]CF_3SO_3^-$.

However, the boron-carbon and carbon-nitrogen bond distances are longer and shorter, respectively, than those of **3**, in line with the weaker electron-donation from boron to the carbene ligand. Compound [$\mathbf{3}^{+\cdot}$]$GaCl_4^-$ is one of very few crystallographically characterized boron radicals (*30*) and molecules featuring boron in the formal +2 oxidation state (*31*). The room-temperature electron paramagnetic resonance spectrum in THF solution displays a complex system (g = 2.0026) because of the couplings with the boron [$a(^{11}B)$ = 6.432 G], hydrogen [$a(^{1}H)$ = 11.447 G], and two nitrogen nuclei [$a(^{14}N)$ = 4.470 G] (fig. S3). The values of spin couplings with the ^{11}B and ^{1}H nuclei are similar to those observed in the persistent $(NHC)BH_2$ radical, whereas the coupling constant with the ^{14}N nuclei is greater than those in the NHC adducts (*32*, *33*), in line with the higher electron-acceptor ability of CAACs versus NHCs. Calculations using the natural bond orbital (NBO) method confirmed that the spin density is mainly located at boron (0.50 *e*) with some contributions of the nitrogen atoms (0.16 *e* and 0.17 *e*). The singly occupied molecular orbital (SOMO) (–7.30 eV) is essentially the boron p orbital, weakly mixing with the p(π) atomic orbital of the two carbene carbons (Fig. 4, right).

Because of the presence of a lone pair of electrons at boron, bis(carbene)BH adduct **3** has the potential to react with electrophiles, which is quite unusual for tricoordinate boron compounds (*5*–*9*, *34*). No reactions of **3** were observed with trimethylsilyl- or methyl-trifluoromethanesulfonate even after heating at 80°C for 14 hours, probably because of the presence of the two bulky CAAC ligands, which shield the boron center. To probe basicity further, we added an equimolar amount of trifluoromethane sulfonic acid to a toluene solution of compound **3** at room temperature, and after work up the conjugate acid [$\mathbf{3H}^+$]$CF_3SO_3^-$ was isolated in 89% yield. The proton-coupled ^{11}B NMR spectrum of this salt shows a triplet (J_{BH} = 83.5 Hz) at –21.8 ppm, confirming the presence of two hydrogen atoms directly bonded to boron and thus the boronium nature (*35*) of [$\mathbf{3H}^+$]$CF_3SO_3^-$. The solid-state structure confirmed the tetracoordination of boron. The boron-carbon and carbon-nitrogen bond distances are in the range of single and double bonds, respectively, in line with the absence of back-donation from boron to the carbene ligand. To quantify the basicity of **3**, we calculated (BP86/def2-SVP+ZPE) its gas phase proton affinity: The 1108 kJ mol^{-1} value is much higher than that calculated for the free BH (856 kJ mol^{-1}) and comparable to the unsaturated free *N*-phenyl–substituted NHC (1107 kJ mol^{-1}) (*36*). In toluene solution, we found that **3** is readily protonated by $BrCH_2CO_2H$, whereas the reaction with $PhCO_2H$ proceeded very slowly, and only trace amounts of [$\mathbf{3H}^+$]$PhCO_2^-$ were detected after 14 hours. Boronium [$\mathbf{3H}^+$]$CF_3SO_3^-$ is rapidly deprotonated by sodium ethoxide in a THF solution, giving back **3** in 68% yield, although no reaction was observed with strong but bulky bases such as potassium hexamethyldisilazide, lithium diisopropylamide, and *t*-butyllithium, confirming the steric shielding of the boron center (*37*, *38*).

Although the parent borylene adduct **3** and the radical cation [$\mathbf{3}^{+\cdot}$]$GaCl_4^-$ are sensitive to air, they are stable at room temperature under argon both in solution and in the solid state for 2 months at least (melting point of **3** is 328°C; [$\mathbf{3}^{+\cdot}$]$GaCl_4^-$, 278°C), which demonstrates the stabilizing efficiency of CAACs. In marked contrast to the well-known tricoordinate boron(+3) derivatives, compound **3**, featuring a boron in the +1 oxidation state, behaves as a Lewis base and can readily be oxidized. Its reactivity with electrophiles is hampered by the bulkiness of the CAAC ligands, but the steric and electronic properties of carbenes can be substantially modulated. Compounds of type **3** are isoelectronic with amines and phosphines, and, because of the lower electronegativity of boron compared to those of nitrogen and phosphorus, they are potential strong electron-donor ligands for transition metals.

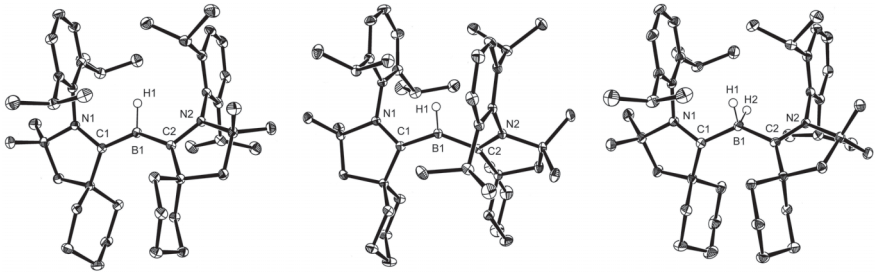

	3	[$\mathbf{3}^{+\cdot}$]$GaCl_4^-$	[$\mathbf{3H}^+$]$CF_3SO_3^-$
B-C (Å)	1.5175(15) [1.535]	1.583(2) [1.575]	1.610(3) [1.617]
	1.5165(15) [1.532]	1.582(2) [1.575]	1.607(3) [1.617]
C-N (Å)	1.3772(13) [1.394]	1.3573(18) [1.357]	1.308(3) [1.334]
	1.3905(13) [1.402]	1.3534(17) [1.354]	1.308(3) [1.334]
C-B-C (°)	138.85(10) [140.1]	137.84(12) [139.6]	133.7(2) [136.4]

Fig. 3. Molecular views (50% thermal ellipsoids are shown) of the parent borylene-bis(CAAC) **3** (left), radical cation $\mathbf{3}^{+\cdot}$ (center), and boronium $\mathbf{3H}^+$ (right) in the solid state (for clarity, H atoms of the carbene ligand and the counterions $GaCl_4^-$ for $\mathbf{3}^{+\cdot}$ and $CF_3SO_3^-$ for $\mathbf{3H}^+$ are omitted). Selected bond lengths (Å) and angles (°) are given in the table; for comparison, the calculated values at the (U)BP86/def2-SVP level of theory are given in brackets.

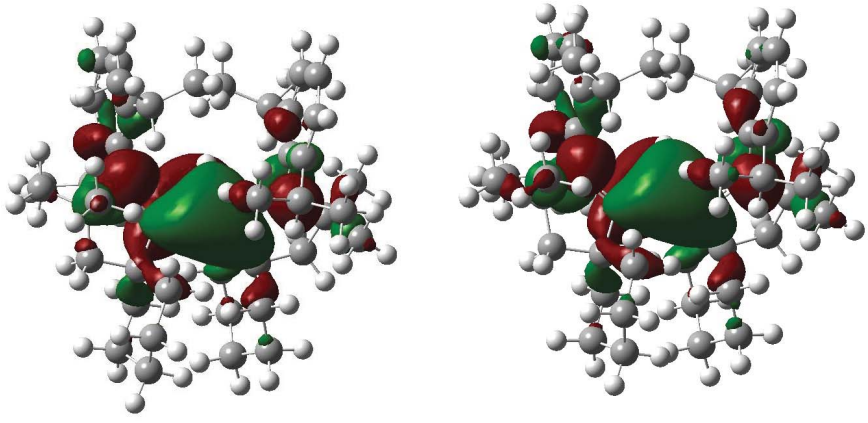

Fig. 4. Plot of the calculated HOMO (–3.34 eV) of the parent borylene-bis(CAAC) **3** (left) and SOMO (–7.30 eV) of the radical cation $\mathbf{3}^{+\cdot}$ (right).

References and Notes

1. R. N. Grimes, *J. Chem. Educ.* **81**, 657 (2004).
2. D. Vidovic, S. Aldridge, *Chem. Sci.* **2**, 601 (2011).
3. M. Yamashita, K. Nozaki, *J. Synth. Org. Chem. Jpn.* **68**, 359 (2010).
4. R. C. Fischer, P. P. Power, *Chem. Rev.* **110**, 3877 (2010).
5. Y. Segawa, M. Yamashita, K. Nozaki, *Science* **314**, 113 (2006).
6. T. B. Marder, *Science* **314**, 69 (2006).
7. H. Braunschweig, *Angew. Chem. Int. Ed.* **46**, 1946 (2007).
8. K. Nozaki, *Nature* **464**, 1136 (2010).
9. M. S. Cheung, T. B. Marder, Z. Lin, *Organometallics* **30**, 3018 (2011).
10. P. Hassanzadeh, L. Andrews, *J. Phys. Chem.* **97**, 4910 (1993).
11. H. F. Bettinger, *J. Am. Chem. Soc.* **128**, 2534 (2006).
12. H. Braunschweig, C. Kollann, U. Englert, *Angew. Chem. Int. Ed.* **37**, 3179 (1998).

13. H. Braunschweig, R. D. Dewhurst, A. Schneider, *Chem. Rev.* **110**, 3924 (2010).
14. F. E. Hahn, M. C. Jahnke, *Angew. Chem. Int. Ed.* **47**, 3122 (2008).
15. D. Bourissou, O. Guerret, F. P. Gabbaï, G. Bertrand, *Chem. Rev.* **100**, 39 (2000).
16. M. Melaimi, M. Soleilhavoup, G. Bertrand, *Angew. Chem. Int. Ed.* **49**, 8810 (2010).
17. Y. Z. Wang, G. H. Robinson, *Chem. Commun. (Camb.)* **2009**, 5201 (2009).
18. D. Martin, M. Soleilhavoup, G. Bertrand, *Chem. Sci.* **2**, 389 (2011).
19. Y. Wang *et al.*, *J. Am. Chem. Soc.* **129**, 12412 (2007).
20. Y. Wang *et al.*, *J. Am. Chem. Soc.* **130**, 3298 (2008).
21. P. Bissinger, H. Braunschweig, K. Kraft, T. Kupfer, *Angew. Chem. Int. Ed.* **50**, 4704 (2011).
22. V. Lavallo, Y. Canac, B. Donnadieu, W. W. Schoeller, G. Bertrand, *Angew. Chem. Int. Ed.* **45**, 3488 (2006).
23. O. Back, B. Donnadieu, P. Parameswaran, G. Frenking, G. Bertrand, *Nat. Chem.* **2**, 369 (2010).
24. G. D. Frey, V. Lavallo, B. Donnadieu, W. W. Schoeller, G. Bertrand, *Science* **316**, 439 (2007).
25. V. Lavallo, Y. Canac, C. Prasang, B. Donnadieu, G. Bertrand, *Angew. Chem. Int. Ed.* **44**, 5705 (2005).
26. Preparation methods and spectroscopic data for compounds **2**, **3**, $[\mathbf{3}^{+\cdot}]GaCl_4^-$, and $[\mathbf{3}H^+]CF_3SO_3^-$ and computational details are available as supporting material on *Science* Online.
27. Attempts to prepare the B-D analog using deuterated toluene as solvent failed, indicating that the hydrogen atom is abstracted from an aryl group of a carbene.
28. M. M. Olmstead, P. P. Power, K. J. Weese, R. J. Doedens, *J. Am. Chem. Soc.* **109**, 2541 (1987).
29. J. Monot *et al.*, *Angew. Chem. Int. Ed.* **49**, 9166 (2010).
30. M. M. Olmstead, P. P. Power, *J. Am. Chem. Soc.* **108**, 4235 (1986).
31. R. Dinda *et al.*, *Angew. Chem. Int. Ed.* **46**, 9110 (2007).
32. T. Matsumoto, F. P. Gabbaï, *Organometallics* **28**, 4252 (2009).
33. J. C. Walton *et al.*, *J. Am. Chem. Soc.* **132**, 2350 (2010).
34. H. Braunschweig, C. W. Chiu, K. Radacki, T. Kupfer, *Angew. Chem. Int. Ed.* **49**, 2041 (2010).
35. W. E. Piers, S. C. Bourke, K. D. Conroy, *Angew. Chem. Int. Ed.* **44**, 5016 (2005).
36. R. Tonner, G. Heydenrych, G. Frenking, *ChemPhysChem* **9**, 1474 (2008).
37. Unsuccessful attempts to deprotonate bis(phosphine)BHX adducts (X: H, Br) were reported (*38*).
38. M. Sigl, A. Schier, H. Schmidbaur, *Chem. Ber.* **130**, 1411 (1997).

Acknowledgments: We are grateful to the NSF (CHE-0924410), U.S. Department of Energy (DE-FG02-09ER16069), and DFG for financial support of this work and to the Japan Society for the Promotion of Science for a postdoctoral fellowship (R.K.). We thank E. Stoyanov for helpful advice in infrared spectroscopy. Metrical data for the solid state structures of **3**, $[\mathbf{3}^{+\cdot}]GaCl_4^-$, and $[\mathbf{3}H^+]TfO^-$ are available free of charge from the Cambridge Crystallographic Data Centre under reference numbers CCDC-822246, CCDC-822247, and CCDC-822248, respectively. The authors and UC Riverside have filed a patent.

Supporting Online Material

www.sciencemag.org/cgi/content/full/333/6042/610/DC1
Materials and Methods
Figs. S1 to S6
Tables S1 and S2
References (*39*–*45*)

27 April 2011; accepted 3 June 2011
10.1126/science.1207573

A Single Molecule of Water Encapsulated in Fullerene C_{60}

Kei Kurotobi and Yasujiro Murata*

Water normally exists in hydrogen-bonded environments, but a single molecule of H_2O without any hydrogen bonds can be completely isolated within the confined subnano space inside fullerene C_{60}. We isolated bulk quantities of such a molecule by first synthesizing an open-cage C_{60} derivative whose opening can be enlarged in situ at 120°C that quantitatively encapsulated one water molecule under the high-pressure conditions. The relatively simple method was developed to close the cage and encapsulate water. The structure of $H_2O@C_{60}$ was determined by single-crystal x-ray analysis, along with its physical and spectroscopic properties.

The unusual properties of bulk water, such as its high boiling and melting points, high dielectric constant, and ability to act as both acid and base, arise from hydrogen bonding in bulk. Clusters of H_2O molecules, both in the gas phase (*1*) and confined in nanoscale spaces defined by the hydrophobic interiors of carbon nanotubes (*2*) or a self-assembled coordination cage (*3*), also undergo hydrogen bonding. However, a single molecule of H_2O without any hydrogen bonding to other organic molecule or coordination to metal is rare so far (*4*).

The inner space of the fullerene C_{60}, which is spherical with a diameter of 3.7 Å, is suitable to entrap a water molecule. When atoms or molecules are encapsulated in fullerenes, it is often possible to control the properties of the outer carbon cage as well as to study the isolated species. Endohedral fullerenes encapsulating a wide variety of species, including metal ions, rare gases, and nitrogen atoms, have been synthesized with physical methods under harsh conditions such as (i) arc discharge of carbon rods containing metal, (ii) ion implantation to empty C_{60} and C_{70}, and (iii) high-pressure and high-temperature treatments of empty fullerenes with rare gases (*5*). However, these methods are not suitable to obtain endohedral fullerenes encapsulating small molecules.

The fourth method for synthesizing endohedral fullerenes is the molecular surgical approach (*6*), which includes construction of an opening on an empty C_{60} or C_{70} cage, insertion of small molecules through it, and then restoration of the original framework, retaining the encapsulated species (*7*). By using such an approach, hydrogen molecules have been entrapped in C_{60} and C_{70} in macroscopic quantities (*8*, *9*). To apply this method to a larger molecule than H_2, developments of synthetic methods are needed to create open-cage fullerenes with an opening large enough for the small molecule to pass through (*10*). Fullerenes with large openings to encapsulate an H_2O molecule have been reported (*11*, *12*), but the encapsulated H_2O is in an equilibrium, with outer H_2O molecules existing in the system in large amounts. Furthermore, attempts to close such large openings have not been reported.

If the size of an opening on fullerenes can be controlled dynamically—that is, a small opening changes into a larger one in situ under specific conditions and regenerates itself again after insertion of a molecule through it—wide varieties of endohedral fullerenes could be synthesized by organic synthesis because restoration of the small opening should be easier than that of the larger one. We report the macroscopic synthesis of $H_2O@C_{60}$ using such a dynamic control of the opening size with a series of organic reactions, as well as the structure and the properties of the molecule in which a molecule of H_2O is completely isolated in a confined space.

The synthetic route for open-cage C_{60} derivatives is outlined in Fig. 1A. Applying our previous synthetic route (*13*, *14*), diketones **3a** and **3b** were synthesized in 29 and 43% isolated yields, respectively, from the reaction of C_{60} with pyridazine derivatives **1a** and **1b** followed by photochemical cleavage of one of the C=C double bonds on the rim of the opening on intermediates **2a** and **2b**, respectively (*15*) (figs. S1 to S12). The lowest unoccupied molecular orbital (LUMO) of open-cage C_{60} with a similar opening motif is mainly located on the conjugated butadiene moiety (*13*), and sulfur (*13*, *14*) and hydrazine derivatives (*11*) were reported to react with that moiety. *N*-Methylmorpholine *N*-oxide (NMMO) is known as a nucleophilic oxidant (*16*), and we found that the reaction of **3** with 2.3 equivalents of NMMO in wet tetrahydrofuran (THF) at room temperature led to the synthesis of **5a** and **5b**, respectively, in good yields after purification with silica gel chromatography (figs. S13 to S18).

The structure of **5a** determined by single-crystal x-ray analysis (Fig. 1B) shows that the opening is constructed by the 13-membered ring containing two hemiacetal carbons, in addition to two carbonyl carbons (table S1). This molecule can be considered as the hydrate of tetraketone **4a** having the 16-membered-ring opening with four carbonyl carbons. Because wet THF was used in this reaction, a water molecule attacked one of the carbonyl carbons in **4a** to give **5a**. When the hydrate **5a** was heated at reflux temperature in toluene for 30 min, complete transformation of

Institute for Chemical Research, Kyoto University, Uji, Kyoto 611-0011, Japan.

*To whom correspondence should be addressed. E-mail: yasujiro@scl.kyoto-u.ac.jp